2014 NDIA GROUND VEHICLE SYSTEMS ENGINEERING AND TECHNOLOGY SYMPOSIUM
MODELING & SIMULATION, TESTING AND VALIDATION (MSTV) TECHNICAL SESSION
AUGUST 12-14, 2014 - NOVI, MICHIGAN

MODELING OFF-ROAD ROLLOVER USING TERRAMECHANICS FOR REAL TIME DRIVING SIMULATOR

Amandeep Singh, PhD
TARDEC- Analytics
US Army
Warren, MI

Dale A Holtz, PhD
Realtime Technologies
Royal Oak, MI

Michael Megiveron
Victor Paul
TARDEC-Motion Base Technologies
US Army
Warren, MI

ABSTRACT

There have been several hundred rollovers in military vehicles in the last decade of deployment, of which approximately fifty percent are fall-based that occur during off-road operations. Off-road fall-based rollovers occur at lower speeds when the soft road gives way underneath the vehicle on one side as the soil is unable to support the vehicle load. During these sudden events, drivers, who are generally not prepared, often make impromptu driving decisions that quickly lead to rollover situations. A real-time driving simulator can be instrumental in reducing rollover incidents when used as a training tool. The current research takes a comprehensive approach in understanding this rollover phenomenon, and develops a novel real-time terramechanics approach with a vehicle dynamics model validated on the N-post shaker. TARDEC's Ride Motion Simulator is then used to examine rollover performance in response to various driving styles under various soil conditions. The results are summarized.

INTRODUCTION

The topic of vehicle rollover has been widely researched over many decades by industry, academia, and the Government [1-3], due to its direct impact on human life. A vehicle is generally considered to have experienced a rollover when tires on one side of the vehicle have lost contact with the ground to the point of no return. The cause for rollover varies depending upon the operating conditions. The most commonly studied on-road rollovers occur at higher speeds and high lateral G's during maneuvers such as obstacle avoidance or J-turns. The vehicle during these rollovers pivots about the outside wheels in response to high lateral G's experienced at the vehicle CG where the outside wheels are laterally constrained by the cornering forces. Many techniques have been established to successfully characterize tire cornering data to accurately model on-road rollovers.

There is another type of rollover condition called fall based rollover that occurs at lower speeds over narrow terrains, near the edge of slopes of the terrains and often times near water. The soil on that side becomes softer and can suddenly break at the

edge, causing the vehicle to rollover (Figure 1). These types of rollovers are more prominent among heavy vehicles with high CGs operating in mountainous regions where roadways are made up of narrow paths with steep side slopes and unstable soil. Many times these difficult terrains offer significant tactical military advantage, and may not be avoided.

In order to improve mobility, vehicles must either be innovatively designed to overcome this issue and/or drivers need to be better trained to out-maneuver these situations. Unfortunately, such experimentations may not be safe and cost effective in the field or at the proving ground. Therefore, real-time driving simulation can be instrumental in learning and developing optimal driving strategies in a safe environment. In the past, TARDEC's Ride Motion Simulator (RMS) has been used to run duty cycle experiments, and evaluate suspension technologies such as Magneto-Rheological dampers [4]. However, these experiments assumed rigid terrains and involved relatively simple steering, acceleration, and braking maneuvers. Using the RMS for a rollover simulation (operating close to the practical limits of the simulator) and that over the soft terrain required a more comprehensive approach. To the best of authors' knowledge, no literature currently exists that covers the fall-based rollover issue. Although research in terramechanics has been active for many decades, most of it addresses straight line mobility.

The current research takes a comprehensive approach starting initially with a rigid terrain assumption. As challenges surface with the rigid terrain assumption, more accurate and efficient terramechanics formulations are developed considering soil displacements over slopes. This research involved the following steps: 1) development of a real-time vehicle dynamics model, 2) development and execution of a representative physical test to validate fall-based roll dynamics of the model, 3) development of a new set of terramechanics equations for the real-time environment, 4) integration of the terramechanics model, the vehicle dynamics model, and the driving simulator, and 5) performance of driver in the loop experiments on TARDEC's RMS over various soil types and slopes.

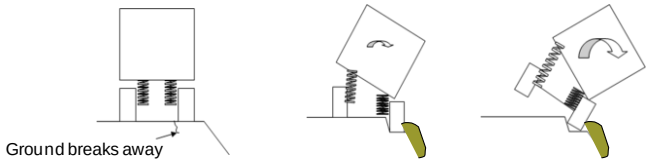

Figure 1: Vehicle rollover due to soil breakaway

FULL VEHICLE DYNAMICS MODELING AND MODEL VALIDATION

A full, multibody vehicle dynamics model was developed using Realtime Technologies Inc.'s Simcreator software [5, 6]. This software is currently used as the simulation framework and real-time vehicle dynamics package in TARDEC's Ground Vehicle Simulation Laboratory (GVSL). The software's vehicle dynamics component library is based on the Composite Rigid Body Methods (CRBM) developed by Walker and Orin [5]. CRBM method is used for the open kinematics chains. To handle closed kinematics chains, constraint equations with corresponding Lagrange multipliers are introduced and are used to augment the dynamics equations with constraint equations. For each constraint equation, a second-order dynamic system is also introduced that minimizes position and velocity errors during the simulation.

The vehicle model that was chosen for this study is of a heavily armored 4x4 currently in the U.S. Army fleet. The vehicle has a double A-arm, independent suspension in both the front and rear. The suspension geometry was validated for kinematics properties such as toe, camber, and roll center height curves. The model's ride and roll stiffnesses were calibrated to known ride frequencies, roll rates, and roll gradient values. Representative center of gravity, mass, and inertial properties were measured utilizing TARDEC's Vehicle Inertial Parameter Estimation Rig (VIPER).

In order to validate roll dynamics for the fall-based simulation, TARDEC's N-post shaker (Figure 2) was employed where the left tires were vertically actuated as a function of time to represent tire paths traced during the soil breakaway condition. The right tires stayed level. As shown in Figure 3, the left profile is determined by three variables: 1) the soil displacement, 2) the rate of fall i.e. the slope of the trajectory, and 3) the vehicle speed which is responsible for the delta time of actuation between the front and the rear tires displacement. Data was collected for both model and the test for the vehicle speeds of 5, 10, and 15 mph, and soil displacements of 4" and 8". The rate of fall was assumed very steep.

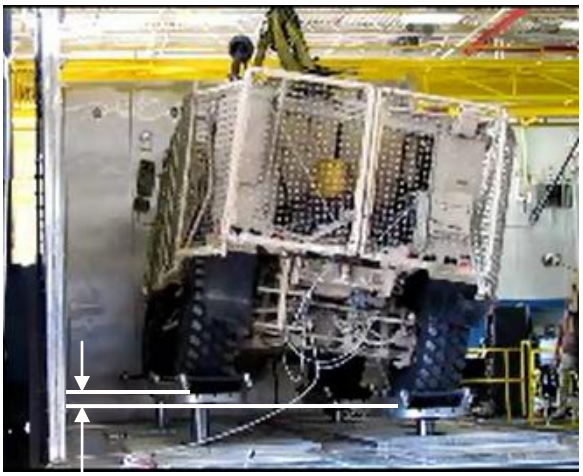

Figure 2: N-post Shaker simulating soil breakaway condition

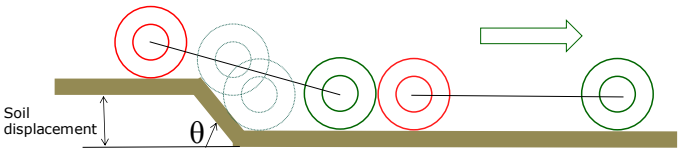

Figure 3: Tire path during soil breakaway.

Figures 4 to 6 compare results from the simulations (blue solid line) against those from the shaker test (red dashed line) for the soil displacement of 8" and the vehicle speed of 10 mph. Figure 4 compares displacements at all the four corner strut locations. Figure 5 compares accelerations in all three directions close to CG. The longitudinal and lateral accelerations do not match that well because of the way the tires were restrained on the shaker. Also, the acceleration components on the shaker were measured with the body-fixed sensors as compared to non-moving reference frame for the simulation. This explains the non-zero value for the lateral acceleration at the end of the test due to vehicle roll angle. The vertical acceleration plot shows good agreement between the model and the test. Figure 6 compares tire vertical forces between the test and the model. The main purpose of this validation is to make sure that the model captured, in general, the behavior as the actual vehicle when subjected to a fall-based situation. Similar correlation was noticed for the other speeds and soil displacements (not shown here).

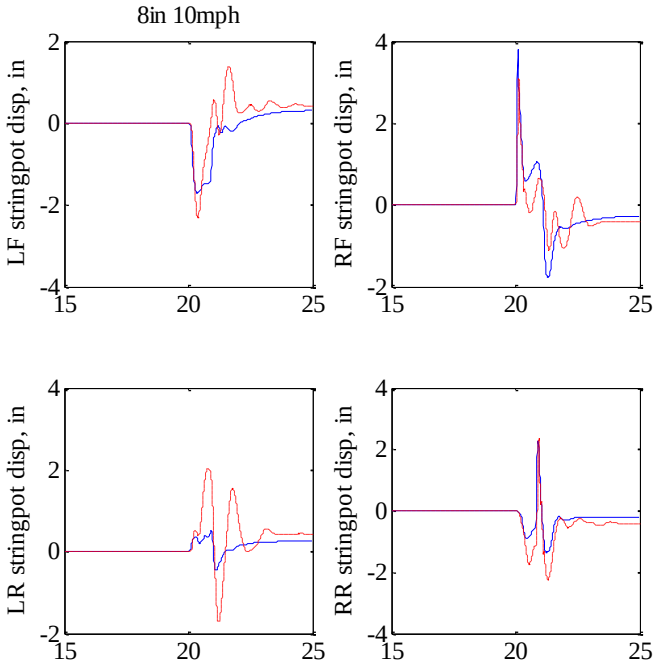

Figure 4: Model (blue) and shaker test (red) displacements at four corners

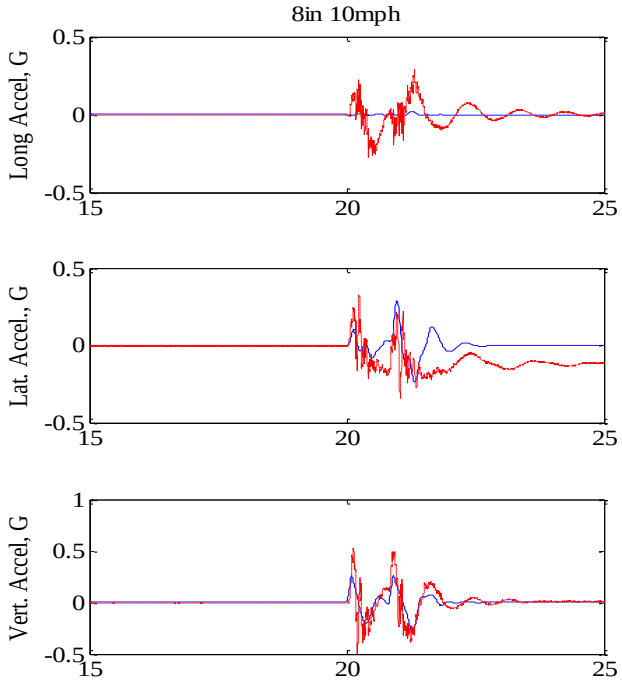

Figure 5: Model (blue) and shaker test (red) vehicle CG acceleration in three directions

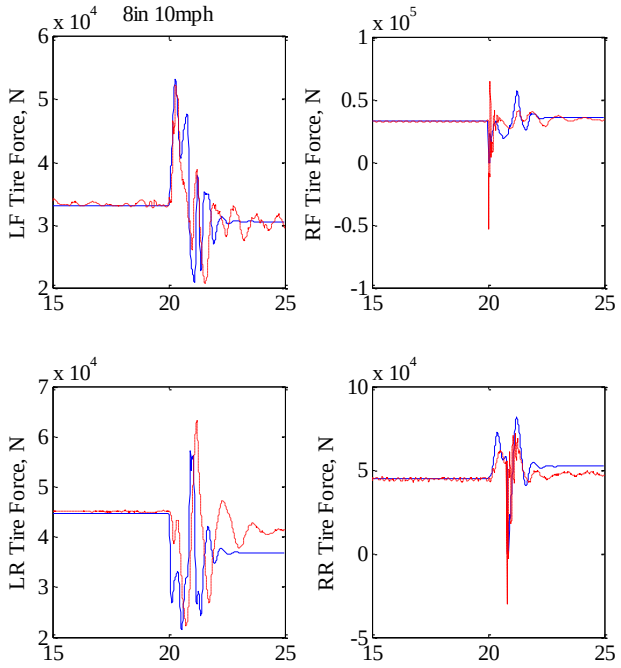

Figure 6: Model (blue) and shaker test (red) tire vertical forces at four corners

Next the model was integrated with the hardware consisting of a steering wheel, a brake pedal, and an accelerator pedal to perform driver in the loop desktop simulations (Figure 7). The steering wheel is connected to a fixed base. In these experiments, the terrain is assumed rigid with slopes on both sides. The soil breakaway on one side is represented by the rigidly deformed profile as shown in Figure 3. The profile represents the "theoretical" path the tires would follow after the soil breaks away. As seen in Figure 8, when the vehicle initially rolled due to sudden lowering of one side, it was pulled to the slope where it slid down but never rolled over. This result was consistent across different combinations of soil displacements, speed, and steering input. Because these early simulations never led to rollover similar to the field, it was concluded that the rigid representation of the soil-breakaway condition was not sufficient for this study, and therefore, an accurate higher fidelity terra-mechanics model was needed. This terramechanics model would require a better representation of the tire contact forces on deformable terrains to produce more accurate vehicle responses during this rollover event.

Figure 7: Desktop simulation set-up

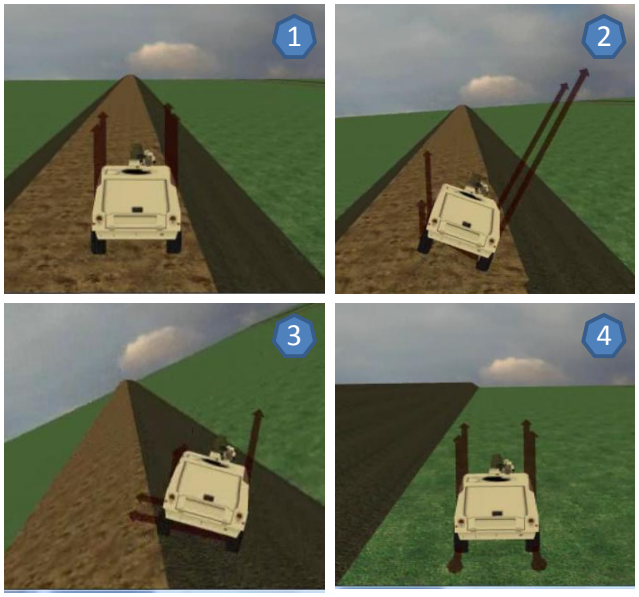

Figure 8: Rigid terrain simulation of soil-breakaway

TERRAMECHANICS MODELING

Terramechanics research has been active for many decades, and therefore, many methods to predict tire-soil interaction are available each with their application and limitations. Three tire-soil interaction methods for flat deformable terrains have been primarily studied for off-road mobility. They are (in the order of complexity) empirical methods [7], semi-empirical methods [8, 9], and finite or discrete element based methods [10,11]. Purely empirical methods based on Bekker's equations, are efficient for general straight-line mobility assessment, but they lack accuracy due to limited parameters. The discrete or finite element based methods are much more accurate but extremely difficult to simulate in a real-time environment. The tire-soil model that was developed for this research uses the semi-empirical method, and is based on the combination of Bekker's equations and the physics based Mohr-Coulomb equations. It computes sinkage into the soil, the lateral and longitudinal forces from the soil deformation, rolling resistance due to the soil compaction, and the lateral plowing effects over lateral slopes. Incorporating Bekker's soil parameters into the model makes it easier to understand what soil parameters affect the rollover performance.

Vertical Force

When a tire drives over soft soil both the tire and the soil will deform. Therefore it is required to simultaneously solve for the tire displacement and the soil sinkage. The vertical stress of the soil, σ can be modeled using Bekker's equation [7]:

$$\sigma = \left(\frac{k_c}{b} + k_\phi\right) z^n \tag{1}$$

where k_c is the cohesive modulus, k_ϕ is the friction modulus, n is the exponent of soil deformation, z is the soil deformation, and b is the width (smallest dimension of the length and width) of the contact area. To get the vertical soil force on the tire, Eq. (1) is multiplied by the area to give

$$F_s = \left(\frac{Ak_c}{b} + Ak_\emptyset\right) z^n \tag{2}$$

Assuming a linear vertical stiffness the vertical tire force can be written as

$$F_t = Kd \tag{3}$$

where K is the stiffness of the tire, and d is the displacement of the tire. Assuming static equilibrium, the forces from Eqs. (2) and (3) must be equal

$$F_s - F_t = 0 \quad \text{or} \quad \left(\frac{Ak_c}{b} + Ak_\phi\right) z^n - Kd = 0 \qquad (4)$$

In addition to Eq. (4), the tire displacement and the sinkage are related by

$$D + z = R - d \quad or\ d = R - D - z \qquad (5)$$

where D is the height of the center of the tire above the terrain, and R is the radius of the tire. After substituting d from Eq. (5) into Eq. (4), z can be solved for using Newton's equation. Solving these equations results in the normal force on the tire (F_t), the tire displacement (d), and the soil sinkage (z). These quantities are used in the following sections to determine the longitudinal and lateral forces and the bulldozing force.

Contact Length

With the tire deformation and sinkage known the contact length between the tire and the soil can be determined. For simplicity, it is assumed that the normal stress is constant over the entire contact region. For this reason, the full sinkage is not used to determine the contact length since at the edges of the tire/soil interface the sinkage will be smaller and the normal stress will be relatively small. Therefore, a conservative value, say, one-fourth of the sinkage is assumed to determine the contact length as follows,

$$L = \sqrt{R^2 - \left(R - d - \frac{z}{4}\right)^2} \qquad (6)$$

For better accuracy, the tire model may be updated to a 3D tire model with non-homogenous stress distribution across the tire patch. However, due to real time simulation demands, a linear tire model has been utilized for this study at this time.

Lateral and Longitudinal Forces

When driving on a soil, the shear strength, τ_{max} of the soil can be approximated using the Mohr-Coulomb equation [12, 15] as,

$$\tau_{max} = c + \sigma \tan\phi \qquad (7)$$

where c is the cohesion, ϕ is the angle of internal friction, and σ is the normal stress. The shear stress can be written in terms of shear displacement [13] as,

$$\tau = \tau_{max}\left(1 - e^{-\frac{j}{K}}\right) \qquad (8)$$

where j is the shear displacement and K is the shear modulus. If a steady state solution is assumed, the shear displacement can be computed from the tire slip. For instance, with a constant slip of i the longitudinal shear deformation can be expressed [14] as,

$$j_x = ix \qquad (9)$$

where x is zero at the front of the tire for forward driving. For a tire with a relatively short contact length, and thus a relatively short time in contact with the soil, this should be an acceptable approximation for most situations. Integrating Eq. (8) over the contact area gives the magnitude of the shear force,

$$F_M = \int_A [c + \sigma \tan\emptyset]\left(1 - e^{-\frac{j}{K}}\right) dA \qquad (10)$$

Depending on the slip angle, tire width, and contact length, the integration of this equation over the contact area of the tire has two possible cases that require a slightly different integration as shown in Figure 9. The tire velocity vector on the contact patch along *EB* determines the slip angle angle, θ, with respect to the plane of the tire *BC*, and *AB* is the front of the tire.

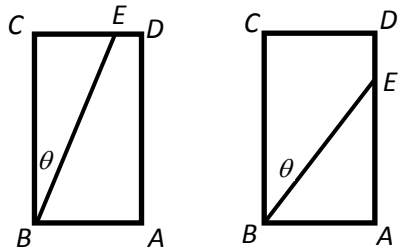

(a) Small Slip Angles **(b) Large Slip Angles**

Figure 9: Soil deformation with small or large slip angles.

For the region *ABED* for the small slip angles and the region *ABE* for the large slip angles, the lateral and longitudinal displacements are

$$j_x = ix \quad and \quad j_y = xtan\theta \tag{11}$$

For the region *BCE* for the small slip angles and the region *BCDE* for the large slip angles, the lateral and longitudinal shear displacements are

$$j_x = \frac{iy}{tan\theta} \quad and \quad j_y = y \tag{12}$$

When computing the shear force in Eq. (10), a combined shear displacement is used

$$j = \sqrt{j_x^2 + j_y^2} \tag{13}$$

For both small and large slip angles, the combined shear displacement is zero at points *A*, *B* and *C* and reach a maximum at points *D* and *E*. After defining j_{max} as the shear displacement at points *D* and *E*, the combined shear for the small slip angle case can be written as

$$j = \frac{j_{max}x}{L} \tag{14}$$

for region *ABDE*, and

$$j = \frac{j_{max}y}{Ltan\theta} \tag{15}$$

for region *BCE*. For the large slip angle case, the combined shear can be written as

$$j = \frac{j_{max}y}{W} \tag{16}$$

for region *ABE*, and

$$j = \frac{j_{max}xtan\theta}{W} \tag{17}$$

for region *BCDE*. Using these definitions of shear displacement for the small slip angle case, Eq. (10) becomes

$$F_M = \int_0^L \int_{xtan\theta}^{W} (c + \sigma tan\emptyset)\left(1 - e^{\frac{-j_{max}x}{LK}}\right) dydx + \int_0^L \int_0^{xtan\theta} (c + \sigma tan\emptyset)\left(1 - e^{\frac{-j_{max}y}{LKtan\theta}}\right) dydx \tag{18}$$

which, on assuming the constant normal pressure over the contact area, becomes

$$F_M = WL\left[1 + \frac{K}{j_{max}}\left(e^{\frac{-j_{max}}{K}} - 1\right)\right] - L^2 \frac{K}{j_{max}} tan\theta \left[\left(1 + e^{\frac{-j_{max}}{K}}\right) + 2\frac{K}{f_a}\left(e^{\frac{-j_{max}}{K}} - 1\right)\right] \tag{19}$$

For the large slip case, Eq (10) becomes

$$F_M = \int_0^W \int_{\frac{y}{tan\theta}}^{L} (c + \sigma tan\emptyset)\left(1 - e^{\frac{-j_{max}y}{WK}}\right) dxdy + \int_0^W \int_0^{\frac{y}{tan\theta}} (c + \sigma tan\emptyset)\left(1 - e^{\frac{-j_{max}xtan\theta}{WK}}\right) dxdy \tag{20}$$

On integration, Eq. (20) becomes,

$$F_M = WL\left[1 + \frac{K}{j_{max}}\left(e^{\frac{-j_{max}}{K}} - 1\right)\right] - \frac{W^2}{tan\theta}\frac{K}{j_{max}}\left[\left(1 + e^{\frac{-j_{max}}{K}}\right) + 2\frac{K}{j_{max}}\left(e^{\frac{-j_{max}}{K}} - 1\right)\right] \tag{21}$$

After the magnitude of the shear force is computed, the longitudinal and lateral tire forces can be computed by assuming the direction of the shear force as a linear function of longitudinal and lateral shear displacements,

$$F_x = F_M \frac{iL}{j_{max}} \quad \text{and} \quad F_y = F_M \frac{Ltan\theta}{j_{max}} \tag{22}$$

for the small slip angle case, and

$$F_x = F_M \frac{iW/tan\theta}{j_{max}} \quad \text{and} \quad F_y = F_M \frac{W}{j_{max}} \tag{23}$$

for the large slip angle case.

Rolling Resistance

The rolling resistance of the tire rolling over soft soil can be divided into two components. The first is the rolling resistance due to the flexing of the tire and is proportional to the tire normal force

$$R_{ct} = F_t c_{RR} \tag{24}$$

where c_{RR} is the rolling resistance coefficient. The second component of rolling resistance is due to the compaction of the soil. This resistance can be written [14] as

$$R_{cs} = \left(\frac{\left(\frac{F_t}{L}\right)^{\frac{n+1}{n}}}{(n+1)\left(k_c + bk_\emptyset\right)} \right) \tag{25}$$

These two components can be combined to give the total rolling resistance

$$R = R_{ct} + R_{cs} \tag{26}$$

Bulldozing Effect

The shear forces calculated in the previous sections do not take into effect the plowing of the soil when a tire is moving sideways. For a blade of depth z pushing on soil the failure of the soil can be shown to occur at an angle of $\frac{\pi}{4} + \frac{\emptyset}{2}$, where ϕ is the friction angle [12], as shown in 10.

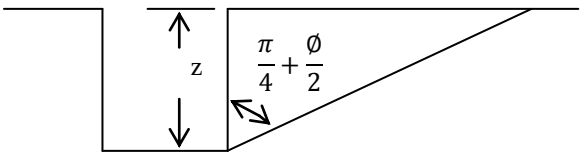

Figure 10: Failure wedge for bulldozing of soil

The force required to achieve failure of the soil [12] is then,

$$F_P = L\left(\frac{\rho g z^2 N_\emptyset}{2} + 2cz\sqrt{N_\emptyset}\right) \tag{27}$$

where ρ is the soil density and g is the gravitational constant. The tire contact length, L, cohesion, c, and sinkage, z, are the same as previously defined. N_ϕ is defined as follows.

$$N_\emptyset = tan^2\left(\frac{\pi}{4} + \frac{\emptyset}{2}\right) \tag{28}$$

The force defined in Eq. (27) is a resistance force that will only oppose motion and will always be zero if the lateral velocity is zero. To approximate this behavior the plowing forces are reduced at low velocities

$$F_P = F_P \frac{v_y}{v_{eps}} \quad \text{if } |v_y| < |v_{eps}| \tag{29}$$

where v_y is the lateral velocity and v_{eps} is a velocity tolerance. The effect of soil build up is not included in F_P and is not considered to be a major effect for the tire because of the relatively short contact length, and the fact that any forward motion of the tire will quickly leave any build up behind. The only case where build up will be an issue is when the tire is moving straight sideways (i.e. a slip angle of $\frac{\pi}{2}$).

FULL VEHICLE DYNAMICS SIMULATION USING TERRAMECHANICS MODEL

The terramechanics model described above is incorporated into the full vehicle model as a C library. The integrated vehicle dynamics model was simulated with J-turn and over a slope to simulate fall-based rollover under varying soil conditions listed in Table 1. The soil properties for Sandy Loam and Dry Sand in Table 1 were taken from [16]. The "Soft" Sandy Loam soil was generated from Sandy Loam by updating the value of exponent of soil deformation from 0.4 to 0.6.

A two step approach was utilized to study the off-road rollover maneuver under various driving conditions:

1. "Off-line" simulations with pre-determined inputs for steering and driving controls to quantify general influence of terramechanics on the vehicle behavior during J-turn and side slope conditions.

2. Real-time driving simulation using the Ride Motion Simulator (RMS) to demonstrate the "feel

factor" in a safe learning environment for Soldiers to improve their driving styles over soft slopes (Figure 11).

Figure 11: Ride Motion Simulator (RMS)

Table 1: Soil properties

	Sandy Loam	Soft Sandy Loam	Dry Sand
Cohesive Modulus Pa-m	11420	11420	990
Friction Modulus, Pa	808960	808960	1528430
Exponent of Soil Deformation	0.4	0.6	1.1
Cohesion, Pa	9650	9650	1040
Friction Angle, deg	35	35	28
Shear Modulus, m	0.2	0.2	0.2
Soil Density, kg/m^3	2000	2000	2000

Offline J-Turn Analysis

A J-turn maneuver was simulated on a flat terrain using different soil properties. During this maneuver, the vehicle speed was increased to about 10 m/s and then, 15 seconds into the maneuver, the steering wheel turned to an angle of 1.0 radian. The maneuver was examined for two different soil properties, Sandy Loam and Soft Sandy Loam from the Table 1. Results are plotted in Figures 12 through 15 for the Sandy Loam properties and indicate a moderate amount of sinkage and bulldozing force. Figure 15 indicates no rollover is experienced.

The J-turn was again simulated over Soft Sandy Loam terrain, and the results are shown in Figures 16 through 19. As seen in the figures, increased soil softness greatly increases the soil sinkage which increases the bulldozing force, enough so that the vehicle rolls over during this maneuver. Figure 19 shows the vehicle roll angle indicating rollover.

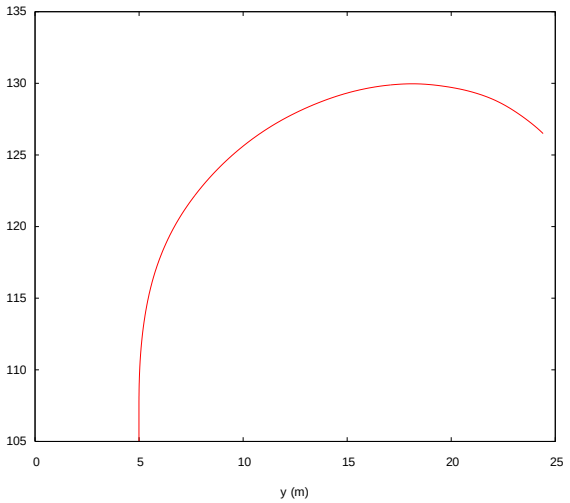

Figure 12: Vehicle path over Sandy Loam soil.

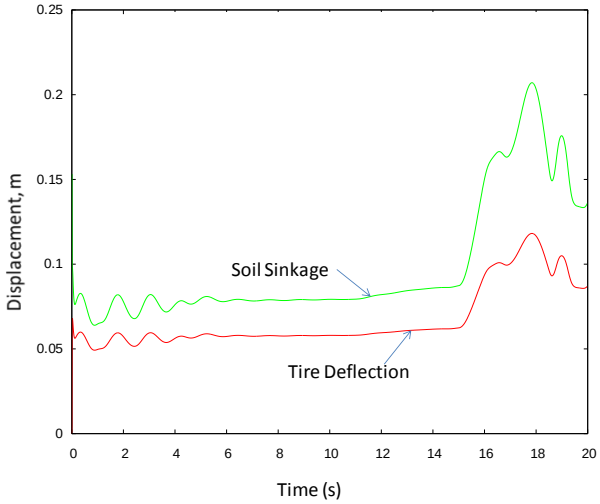

Figure 13: Tire/Soil displacement (Sandy Loam)

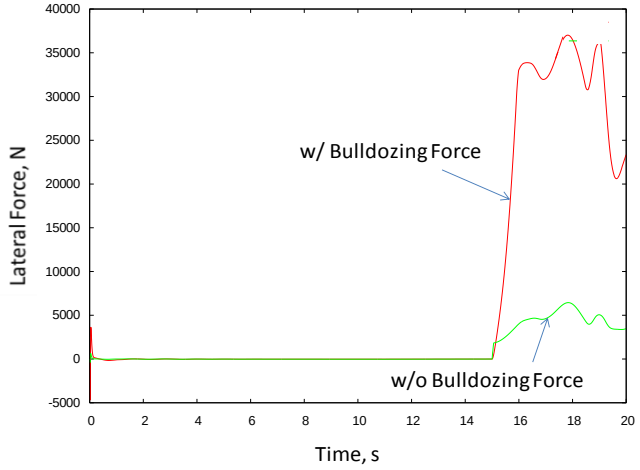

Figure 14: Tire lateral forces (Sandy Loam)

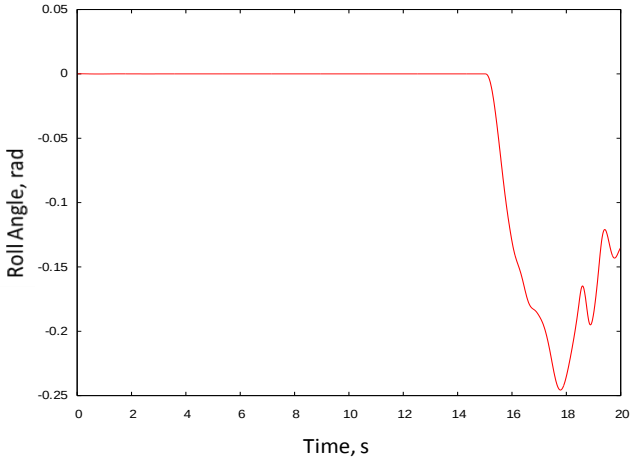

Figure 15: Vehicle roll angle (Sandy Loam)

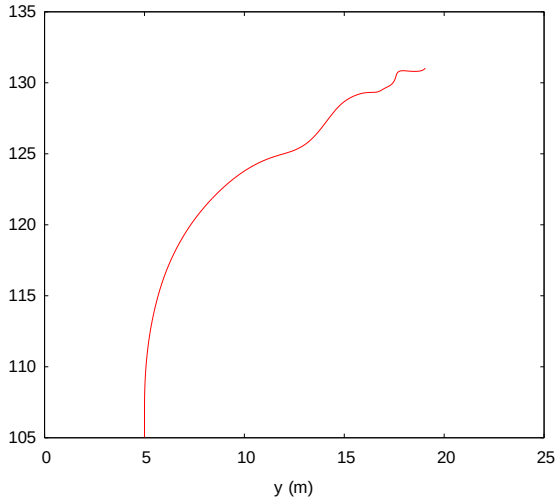

Figure 16: Vehicle path over Soft Sandy Loam

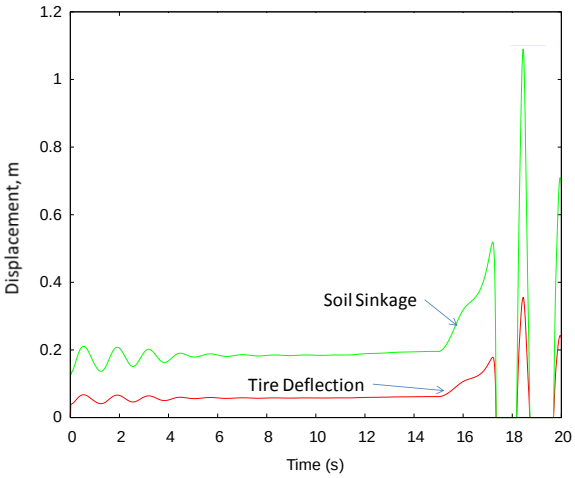

Figure 17: Tire/Soil displacement (Soft Sandy Loam)

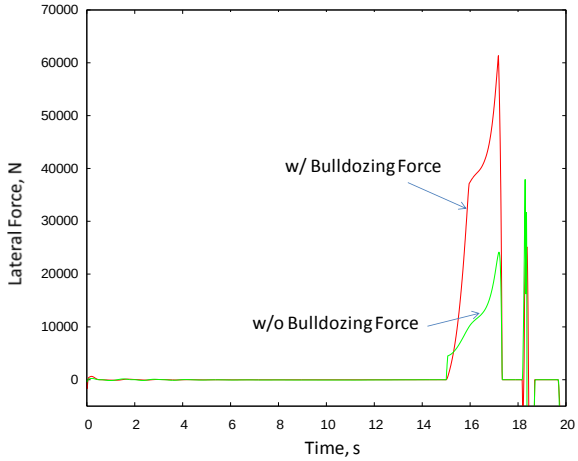

Figure 18: Lateral forces (Soft Sandy Loam)

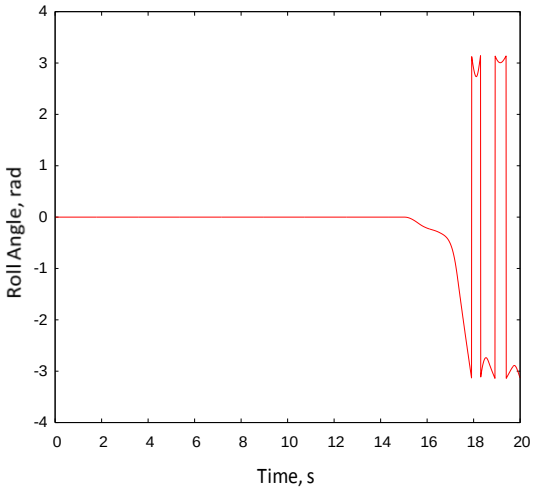

Figure 19: Vehicle Roll angle (Soft Sandy Loam)

Offline Fall-based Rollover Analysis in a Slope

Fall based rollovers occur when the vehicle is traveling near the edge of a terrain with a severe side slope on either side. The soil near the edge of the road (slope side) is often softer than the rest of the roadway, and can sometimes break under the tires of heavy vehicles. When this happens, one side of the vehicle suddenly drops down causing the vehicle to be pulled sideways down the slope. To simulate this condition, the vehicle model was driven on a flat terrain with large slopes on both the left and right sides as shown in Figure 20. During the simulations, the vehicle would start on the flat region and was controlled onto one of the sloped regions. Different soil properties from Table 1 were used on the flat region and both sloped regions. The flat region used the soil properties of "Sandy Loam", while the left and right slopes were set-up with the properties of "Soft Sandy Loam", and "Dry Sand" respectively. The vehicle rollover performance was examined first over the Soft Sandy Loam slope (left slope), and then over the Dry Sand (right slope) for comparison. A speed controller was used to bring the vehicle to a predefined speed and was turned off when the front left tire reached the sloped region.

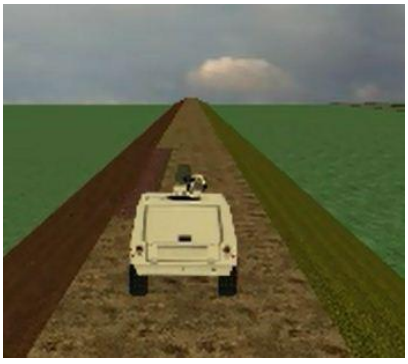

Figure 20: Vehicle starting on a flat region

Table 2 shows the results for Soft Sandy loam slope (left side) for different vehicle speeds and different slope angles. It can be seen that the vehicle rolls over for slopes more than 0.4 rad (~23 deg). Figure 21 shows the vehicle experiencing rollover on a slope of 0.6 rad. (Note that the vehicle shown in the Figure 21 is for graphical purposes only, and does not in any way represent the performance presented here.)

Table 2. Slope maneuver with Sandy Loam soil properties

θ, rad	Vehicle Speed		
	5 m/s	10 m/s	15 m/s
0.2	Slide	Slide	Slide
0.3	Slide	Slide	Slide
0.4	Slide	Rollover	Rollover
0.5	Rollover	Rollover	Rollover
0.6	Rollover	Rollover	Rollover

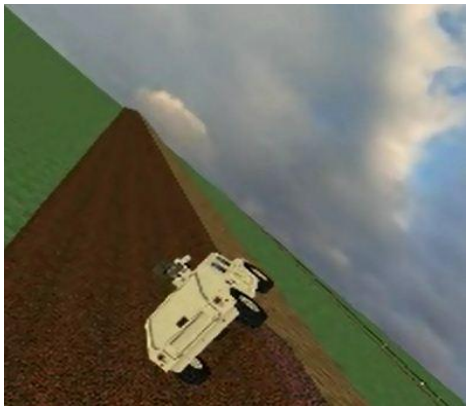

Figure 21: Vehicle rolls over soft sandy loam@0.6 rad slope

Typically, when a driver gets pulled into a slope, their natural reaction is to quickly steer back to the flat terrain. On simulating this condition, it was found that such a steering "correction" might actually contribute to rollover situations. This condition was simulated using Soft Sandy Loam soil properties but with a steering wheel turn of 0.25 rad (14.3 deg) back toward the flat region of the terrain, triggered after the front left wheel has reached 2 m down the slope. According to Table 3, it is seen that a small steering correction to return to the flat terrain actually increases the chance of rollover. In that case, steering the opposite way i.e. going down the slope may perhaps be better to avoid rollover. Further, results indicate that increased vehicle speed with steering also increases potential for vehicle rollover.

Table 3. Slope with steering of 14.3 deg

θ, rad	Vehicle Speed		
	5 m/s	10 m/s	15 m/s
0.2	Slide	Slide	Rollover
0.3	Slide	Rollover	Rollover
0.4	Rollover	Rollover	Rollover
0.5	Rollover	Rollover	Rollover
0.6	Rollover	Rollover	Rollover

In order to demonstrate the importance of modeling lateral bulldozing forces, simulations were re-run with the same soil properties and steering input but with bulldozing force disabled. Table 4 shows that the vehicle doesn't rollover on the slope but slides down for all the cases when bulldozing forces are not included. Finally, Table 5 shows no rollover on the slope but slide when simulated using Dry Sand soil properties from Table 1 with bulldozing force and steering activated (Figure 22).

Table 4. Slope without bulldozing forces

θ, rad	Vehicle Speed		
	5 m/s	10 m/s	15 m/s
0.2	Slide	Slide	Slide
0.3	Slide	Slide	Slide
0.4	Slide	Slide	Slide
0.5	Slide	Slide	Slide
0.6	Slide	Slide	Slide

Table 5. Slope with dry sand

θ, rad	Vehicle Speed		
	5 m/s	10 m/s	15 m/s
0.2	Slide	Slide	Slide
0.3	Slide	Slide	Slide
0.4	Slide	Slide	Slide
0.5	Slide	Slide	Slide
0.6	Slide	Slide	Slide

Figure 22: Vehicle slide over a dry sand slope @0.6 rad

RIDE MOTION SIMULATOR (RMS) EXPERIMENTS

The RMS, shown in Figure 11, is a single occupant simulator with a 40Hz acceleration bandwidth capable of producing linear accelerations of ±2g's and angular accelerations of ±1150°/sec2. It can be used to reproduce the ride of any vehicle whether wheeled or tracked. The simulator was configured with a LCD screen for visuals, a speaker system for vehicle sounds, a steering wheel, and pedals. One of the major difficulties in motion based driving simulation recreating sustained accelerations due to the limited motion envelope of the simulator. The RMS has a linear range of ±0.5m and an angular range of ± 20°. In order to provide the RMS' occupant with the sensation of sustained acceleration, as you would experience in a vehicle, the RMS relies on motion cueing algorithms that provide the occupant with initial onset acceleration and then replaces linear accelerations with angular displacements. For instance when the driver makes a right turn the simulator will move left and roll right.

For this exercise, the vehicle is first driven over the flat rigid terrain to validate roll and steering feel in general. Then, experiments were conducted on the left slope with soft sandy loam followed by similar experiments on the right slope with dry sand properties. The vehicle speed of entry was maintained between 10 and 15 mph. As noted in the list below, Experimental runs E1-E4 were conducted on the Soft Sandy loam slope on the left side, while Experiments runs E5-E9 were conducted on the Dry

Sand on the right side. A list of the conditions of each experimental run are given below:

Soft Sandy Loam conditions-

E1. Immediate counter steering to get back to the flat region as soon as the rolling over is sensed
E2. No steering action to represent "deer in the headlight" scenario.
E3. Immediate steering to get down the slope as soon as rolling is sensed with "throttle on"
E4. Immediate steering to get down the slope as a soon as rolling is sensed with foot off the throttle

Dry Sand conditions-

E5. No steering action to represent "deer freeze"
E6. Counter steering correction to get back on to the slope as soon as rolling is sensed
E7. Immediate steering down to get down the slope with full throttle on
E8. Immediate steering down to get down the slope without throttle
E9. Delayed steering down to get down the slope
E10. Quick steering down the slope as soon as rollover possibility is sensed

Following intermediate observations were made with results noted in Table 6:

1. Soil properties can influence "where" the rollover may occur either "on" the slope or at the "end" of the slope. A vehicle would tend to slide down the dry sand slope (E5-E10) without rolling over whereas the vehicle may rollover "on" the slope with soft Sandy Loam. This is because dry sand cannot generate enough lateral shear force or bulldozing force to constrain the tire motion to cause enough rolling moment.

2. A counter steering correction to get the vehicle back to the flat may worsen the rollover situation on a soft Sandy Loam slope (E1).

3. Immediate steering to drive the vehicle down the slope as soon as impending rollover is sensed may reduce the rollover potential on the soft sandy loam slope (E3).

4. A vehicle on a dry sand slope may still rollover on hitting the ground at the end of the slope after sliding. It was determined that it is very challenging to influence the vehicle dynamics of a sliding vehicle with any steering strategy. However, immediate steering early-on near the edge of the slope may reduce rollover potential (E10).

5. Pushing the throttle at the end of the slope seems to help in reducing the rollover potential (E7). More studies need to be done to understand this better.

Table 6. Driving Simulator Experiments

Driving Simulator Experiment	Soil Type	Outcome on the Slope	Outcome at the end of the Slope
E1	Soft Sandy Loam	Rollover	-
E2		Rollover	-
E3		No rollover	No rollover
E4		No rollover	No rollover
E5	Dry Sand	Slide	Rollover
E6		Slide	Rollover
E7		Slide	No Rollover
E8		Slide	Rollover
E9		Slide	Rollover
E10		Slide	No rollover

CONCLUSIONS

A full vehicle model was developed using a real-time simulation code. The model was validated for roll dynamics using the N-post shaker represented by a rigid terrain profile. A novel semi-empirical terramechanics model with lateral bulldozing force effect was also developed and integrated into the full-vehicle model. The vehicle model was simulated in real-time, and the effects of various parameters including vehicle speed, soil properties, terrain slope, and bulldozing forces were investigated. It was found that soil properties and bulldozing forces play an important role in causing vehicle rollover. Driving simulator experiments and off-line simulations determined steering and throttle strategies that can help Soldier reduce rollover incidents. Further, work with a variety of drivers, vehicle models, and steering scenarios may be needed to improve the generalization and theoretical explanation of rollover mitigation.

ACKNOWLEDGMENTS

Authors would like to thank the following TARDEC Physical Simulation Lab associates: Harry Zywiol for providing leadership support for using their driving simulator, and Bill Meldrum and Melissa Morgan for the shaker testing support. Also, thanks to Prof. Paul Ayers, University of Tennessee for initial guidance on soil bulldozing effects.

REFERENCES

1. Winkler, C., "Rollover of Heavy Commercial Vehicles," *University of Michigan Transportation Research Institute Report*, ISSN 0739 7100, 2000.
2. Hac, A., "Detection of Vehicle Rollover," *Proceedings of SAE World Congress*, #2004-01-1757, 2004.
3. Peters, S., Iagnemma K., "Stability Measurements of High Speed Vehicles," *Vehicle System Dynamics*, 47-6, p701-720, 2009.
4. Megiveron, M., Singh, A., "Real-time driving simulation of magneto-rheological active damper Stryker suspension," *Proceedings of the Society of Automotive Engineer World Congress*, Detroit, MI, 2012.
5. Romano, R., "Real-time Multibody Vehicle Dynamics using a Modular Modeling Methodology," *Proceedings of SAE World Congress*, paper # 2000-01-1297, 2000.
6. Romano, R., Schultz, S., "Validation of Real-time Multi-body Vehicle Dynamics Models for Use in Product Design and Acquisition," *Proceedings of SAE World Congress*, Paper #2004-01-1582, 2004.
7. Bekker, M. G., *Off-the Road Locomotion*, University of Michigan Press, 1960.
8. Wong, J., Y., "Terramechanics and Off-road Vehicle Engineering Terrain Behaviour, Off-road Vehicle Performance and Design," *ScienceDirect-online*, Elsevier, 2010
9. Madsen, J., D. Negrut, A. Reid, A. Seidl, P. D. Ayers, G. Bozdech, J. Freeman, and J. O'kins, "A Physics-based Vehicle/terrain Interaction Model for Soft Soil Off-road Vehicle Simulations," *SAE Journal of Commercial Vehicles*, 5:280-290, 2012.
10. Shoop, S. A., "*Finite Element Modeling of Tire-Terrain Interaction*," PhD Dissertation, University of Michigan, 2001.
11. Nakashima, H., Oida, A., "Algorithm and implementation of soil-tire contact analysis code based on dynamic FE-DE method," *Journal of Terramechanics*, 41(2), pp. 127-137, 2004.
12. Das, B. M., *Principles of Geotechnical Engineering*, Fifth Edition, Pacific Grove, 2002.
13. Janosi, Z., & Hanamota, B., "The analytical determination of drawbar pull as slip for tracked vehicles in deformable soils," *1st International Conference on the Mechanics of Soil-Vehicle Systems*, Torino, Italy, 1961.
14. Laughery, S., Gerhart, G., & Muench, P., "Evaluating Vehicle Mobility Using Bekker's Equations," *US Army Report*, Warren, MI, 2000.
15. McKyes, E., *Soil Cutting and Tillage*, Elsevier Science Publishing Company, New York, 1986.
16. Wong, J., Y., *Theory of Ground Vehicles*, John Wiley & Sons, 4th Edition, pp. 130, 2008.